Available online at www.sciencedirect.com

SCIENCE DIRECT®

Remote Sensing of Environment 93 (2004) 546–564

Remote Sensing of Environment

www.elsevier.com/locate/rse

AVHRR-based mapping of fires in Russia: New products for fire management and carbon cycle studies

Anatoly I. Sukhinin, Nancy H.F. French*, Eric S. Kasischke, Jenny H. Hewson, Amber J. Soja, Ivan A. Csiszar, Edward J. Hyer, Tatiana Loboda, Susan G. Conrad, Victor I. Romasko, Eugene A. Pavlichenko, Sergey I. Miskiv, Olga A. Slinkina

Environmental and Emerging Technologies Division, Altarum Institute, 3520 Green Court, Suite 300, Ann Arbor, MI 48105, United States

Received 12 November 2003; received in revised form 17 June 2004; accepted 22 August 2004

Abstract

A new database of fire activity in Russia derived from 1-km resolution remote sensing imagery is presented and discussed. The procedure used to generate this burned-area product is described, including active-fire detection and burn-scar mapping approaches. Fire detection makes use of a probabilistic procedure using image data from the United States National Oceanic and Atmospheric Administration's (NOAA) advanced very high resolution radiometer (AVHRR) system. Using the combination of AVHRR data collected at the Krasnoyarsk, Russia, high-resolution picture transmission (HRPT) receiving station, and data from the NOAA Satellite Active Archive (SAA), fire maps are being created for all of Russia for 1995 to 1997 and all of Eastern Russia (east of the Ural Mountains) for 1995 to 2002. This mapping effort has resulted in the most complete set of historic fire maps available for Russia. An initial validation indicates that the burned-area estimates are conservative because the approaches do not detect smaller fires, and, in many cases, fire areas are slightly underestimated. Analyses using the fire database showed that an average of 7.7×10^6 ha yr^{-1} of fire occurred in Eastern Russia between 1996 and 2002 and that fire was widely dispersed in different regions. The satellite-based burned-area estimates area were two to five times greater than those contained in official government burned-area statistics. The data show that there is significant interannual variability in area burned, ranging between a low of 1.5×10^6 ha in 1997 to a high of 12.1×10^6 ha in 2002. Seasonal patterns of fire are similar to patterns seen in the North American boreal region, with large-fire seasons experiencing more late-season burning (in August and September) than during low-fire years. There was a distinct zonal distribution of fires in Russia; 65% of the area burned occurred in the taiga zone, which includes southern, middle, and northern taiga subzones, 20% in the steppe and forest steppe zones, 12% in the mixed forest zone, and 3% in the tundra and forest-tundra zones. Lands classified as forest experienced 55% of all burned area, while crops and pastures, swamps and bogs, and grass and shrubs land cover categories experienced 13% to 15% each. Finally, the utility of the products is discussed in the context of fire management and carbon cycling.

Keywords: forest fire; NOAA AVHRR; fire detection and mapping; Russia

1. Introduction

The need for a consistent, broad-scale approach to mapping fires globally has led to several recent initiatives to detect and characterize fire using satellite remote-sensing systems (Arino et al., 2001; Barbosa et al., 1999; Eva & Lambin, 1998; Fraser et al., 2000; Grégoire et al., 2003; Justice et al., 2002; Li et al., 2000; Roy et al., 2002; Stroppiana et al., 2000; Sukhinin, 2003). The documentation of when and where fire has occurred is important for understanding fire's impact on the land and atmosphere. Fire and land managers need accurate maps of past fire so they can manage the landscape. Climate researchers are interested in quantifying burned area to understand how emissions from fire affect the atmosphere. Programs such as the International Geosphere–Biosphere Program (IGBP)

* Corresponding author. Tel.: +1 734 302 4719; fax: +1 734 302 4991.
E-mail address: nancy.french@altrarum.org (N.H.F. French).

0034-4257/$ - see front matter © 2004 Elsevier Inc. All rights reserved.
doi:10.1016/j.rse.2004.08.011

and Global Observation of Forest and Landcover Dynamics (GOFC/GOLD), an international program under the Global Terrestrial Observing System (GTOS), have encouraged an integrated and comprehensive accounting of global fire and have promoted the use of remote sensing methods (Ahern et al., 2001; Kasischke & Penner, 2004). The extensive area and remote nature of much of boreal Russia make remote sensing an important source of information for studying fire and the consequence of fire in this region.

In this paper, we present a new database containing estimates of burned area in Eastern Russia derived from 1-km resolution remote sensing imagery from the United States National Oceanic and Atmospheric Administration's (NOAA) advanced very high resolution radiometer (AVHRR) system. The database currently includes fire location and burned-area maps within the acquisition mask of a direct-readout receiving station located in Krasnoyarsk in Central Russia (55°59 N, 92°41′ E) and 3 years of data for an extended region of Eastern Russia (Fig. 1) derived using additional AVHRR data from the NOAA archives. For the final products, we plan to map all fires in the boreal region of Russia, east of the Ural Mountains, from 1995 through 2002 and fires in all of Russia, including Western (European) Russia, for 1995 to 1998 using a consistent fire-detection methodology. Previous, less extensive versions of this database have been presented and used in analyses to understand the impact of fire on the Russian boreal forest (Conard et al., 2002; Kasischke & Bruhwiler, 2002; Soja et al., 2004a, 2004b; Sukhinin, 2003). The current version of this database, which covers a broader region than did previous versions and includes several years of additional information, is now being released for general use (http://www.glcf.umiacs.umd.edu/data/russiaforest/). Our purpose in this paper is to present and describe the production of the data products, to show examples of this new set of historical fire maps, and present the results of preliminary analyses of the data. Included is a discussion of the products' strengths and inconsistencies, as well as their potential utility in fire management and carbon cycle science. We conclude that this new data set offers extended utility over other fire products available for the region for quantifying the burned area in this fire-prone region of the Earth.

2. Background

Disturbance by wildfire is common in the circumpolar boreal forest region, especially in the continental regions of North America and Russia. The forests of this region are dominated by conifer ecosystems—pine and spruce in North America, larch and pine in Eurasia—which hold large amounts of carbon aboveground, in the forest floor, and in soils (Van Cleve et al., 1986; Shugart et al., 1992; Kasischke, 2000; Stolbovoi, 2002). On average, some 2.5×10^6 ha (25,000 km^2) of land burn each year in the North American boreal forest, with as much as 7.0×10^6 ha burning during high-fire years (French et al., 2000; Stocks et al., 2002). The incidence of fire in Russia is less well known because of inaccuracies in official burned-area statistics (Conard & Ivanova, 1997). For example, official Russian estimates of annual burned area ranged from 0.23 to 5.4×10^6 ha yr^{-1} between 1980 and 1999 (Korovin, 1996; Shvidenko & Goldammer, 2001), where satellite estimates range between 1.5 and 11.7×10^6 ha yr^{-1} (Cahoon et al., 1994, 1996; Soja et al., 2004b).

The forests of Russia represent a significant national resource and have been systematically inventoried (since 1961) and managed for forest products in the more productive and accessible regions (Kukuev et al., 1997; Shvidenko & Nilsson, 2002). Historically, 60% of the forest

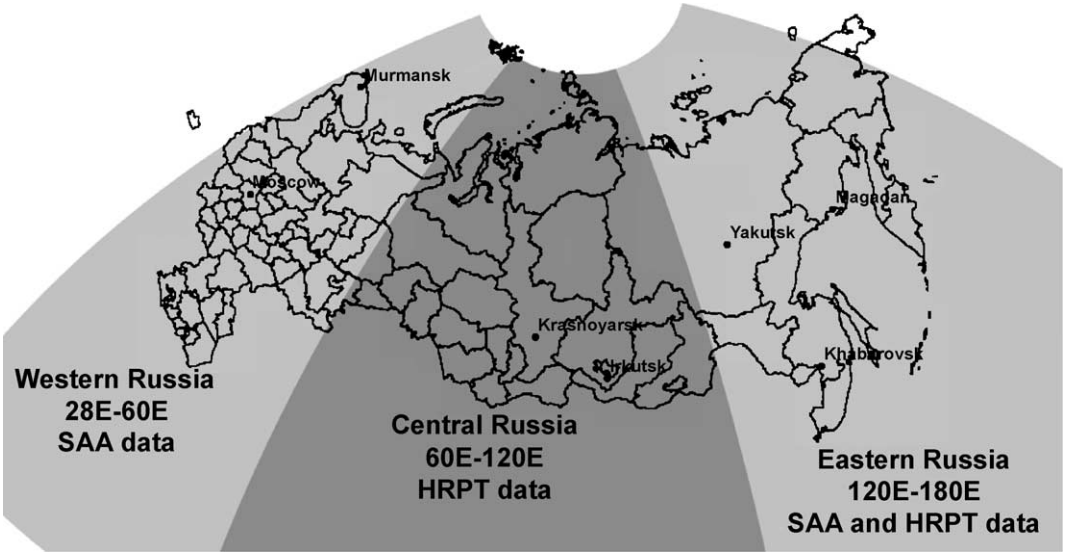

Fig. 1. Map of Russia showing the regions of coverage and location of Krasnoyarsk, the site of the high-resolution picture transmission (HRPT) receiving station used for fire mapping.

has been monitored (protected) to aid in fire management and suppression. Fire suppression is carried out at the Federal level using ground and aerial methods through the National Forest Fire Center of Russia. The area of this protected zone varies from year to year and has been considerably smaller in recent years. This is because economic constraints have resulted in a lowering of fire suppression activity, with many fires not being controlled or managed in ways desired for optimal forest production (Goldammer & Stocks, 2000). In the unprotected zone, fire has never been and is not currently controlled or documented (Shvidenko & Nilsson, 2000; Sofronov et al., 1998).

Due to its vast land area, the frequency of fire, and limitations on management resources, the need for broad-scale remote sensing-based monitoring of fire in the whole of Russia is evident. To meet this need, a team of experts from Avialesookhrana (the Central Aviation Base of Russian Forest Defense Service), the Space Research Institute (Moscow), the Center of Forest Ecology and Productivity (Moscow), and the Institute of Solar-Terrestrial Physics (Irkutsk) has joined efforts to develop a national, satellite-based fire data acquisition and distribution system using Internet resources (http://www.nffc.aviales.ru/engl/main.htm). Regional monitoring systems have also been developed at various institutions that operate direct-readout receiving stations. Both the national and regional systems are used by fire managers.

Russia's boreal forests cover an estimated 835 to 896×10^6 ha and hold 28% of the world's terrestrial carbon in the forests and soils (Apps et al., 1993; Dixon et al., 1994; Kasischke, 2000; Shvidenko & Nilsson, 2002). With such high-carbon reserves, regional issues related to carbon cycling become globally important, and several efforts have been undertaken to study the impact of fire on this large carbon pool. An important piece of information required for quantifying fire's impact is the occurrence and location of fire. Past efforts on quantifying the direct emission of carbon from biomass burning have used fire statistics compiled at regional scales (Seiler & Crutzen, 1980), while more recent efforts have used spatially explicit data to assess the impact of fire (Amiro et al., 2001; Conard et al., 2002; French et al., 2000, 2002; Kajii et al., 2002, Kasischke & Bruhwiler, 2002; Soja et al., 2004a,). Because of the incomplete record of fire in the Russian boreal region, these efforts have resulted in a wide range of carbon emission estimates. Improvement in estimates of area burned is the first step for improved accuracy in fire emissions from this region (French et al., 2004).

AVHRR data are unique resource for fire monitoring and mapping because they have provided continuous daily global coverage for more than two decades and have been extensively used for fire mapping in many biomes (Barbosa et al., 1999; Cahoon et al., 1994, 1992; Fraser et al., 2000; Kasischke & French, 1995; Razafimpanilo et al., 1995; Remmel & Perera, 2001; Siegert & Hoffmann, 2000; Stroppiana et al., 2000). In some areas, fire is also monitored daily with AVHRR and made available to scientists and forest managers through web-based information systems (see http://www.fire.uni-freiburg.de/ and http://www.gofc-fire.org). Two general categories of products are typically derived from AVHRR data: fire hot spot detection maps using the thermal bands, and burned-area maps using multiple bands of postfire images. In some cases, such as the products described in this paper, improved estimates of area burned have been made using a hybrid algorithm that combines hot spot detections with burn area maps. Fraser et al. (2000) present a review of AVHRR fire detection and mapping research and describe a hybrid technique that they have developed for fire mapping in Canada.

Despite this extensive use of AVHRR for fire monitoring and mapping, this sensor was not designed for fire detection and is not optimally configured for this application. In particular, the mid-infrared thermal band of AVHRR at 3.7 μm saturates at ~322 K for AVHRR/2 (up to NOAA-14; Csiszar & Sullivan, 2002) and ~335 K for AVHRR/3 (NOAA-15 and onwards) and can also be contaminated by solar reflectance if daytime images are used. Such brightness temperatures are often reached when only a small fraction of the pixel contains flaming fires. This makes it impossible to accurately quantify fire size and energy from AVHRR for a broad range of fires. In addition, small or low-intensity fires may not be detected due to sensor resolution and the response time (Point Spread Function) of the instruments (Cahoon et al., 2000). The switch of band 3 of the AVHRR/3 sensor from a wavelength of 3.7 μm at night to 1.6 μm for daytime overpasses over many areas and time periods has severely limited the utility of the instrument for daytime active-fire detection. Because of these limitations, issues related to the heterogeneity of the AVHRR long-term time series remain (Csiszar et al., 2003). Nevertheless, AVHRR is the longest global data set available for fire mapping (Gutman et al., 2001) and represents a unique source of fire information in areas of the globe where land-cover changes have been poorly documented, such as the remote regions of Siberia.

3. Methods

3.1. Image data and region of coverage for mapping fires

For this study, we used image data collected by the NOAA AVHRR instruments. In 1995, NASA installed a high-resolution picture transmission (HRPT) receiving station (built by the U.S. Quorum Communication) at the Sukachev Forest Institute in Krasnoyarsk in central Siberia to directly receive 1.1-km resolution AVHRR data from NOAA satellites. The NOAA-12, -14, -15, and -16 satellites have supplied AVHRR data to the Krasnoyarsk station since its installation. In addition, local area coverage (LAC) and archived HRPT data from other stations (1.1-km resolution at nadir) were analyzed.

Imagery collected at the Krasnoyarsk HRPT receiving station is the primary data used to produce the fire data set presented in this paper. Product version A (V_A) is a data set derived from the original and ongoing collections at the Krasnoyarsk HRPT station (Table 1). The station obtains images from satellite passes covering a region from approximately 52° to 157° E longitude and the entire latitudinal extent of Russia, and covers Russia from the Ural Mountains to the Far East (Central and Eastern Russia). However, image data from the edges of the AVHRR collection mask (east of 120° E longitude) are often unusable due to low satellite elevation angle at the receiving station and consequent attenuation of the HRPT transmission (Fig. 1). For this study, every daytime image (daytime lasts approximately 16 h of each day during summer months) was downloaded and processed during fire seasons, which can extend from April through October. Daytime imagery is desired for active-fire detection because daily temperature and fuel moisture conditions translate to more fires starting during the daylight hours. The Krasnoyarsk HRPT station receives images from approximately four satellite overpasses each day. The initial fire products of fire within the Krasnoyarsk HRPT acquisition area were created starting in 1995 and continued though the 2002 fire year (product version A1—V_{A1}; Table 1).

Additional AVHRR data were acquired from the NOAA Satellite Active Archive (SAA) to improve fire detection and mapping at the edges of the station's collection region, to extend the coverage to the extreme eastern region of Russia, and to augment data for early years within the station collection region (1995 to 1997). These were provided to the Krasnoyarsk-based analysts for production of the second version of fire database products (product V_B; Table 1). For the region from approximately 120° to 180° E longitude, between 80 and 100 AVHRR images for each 2-week period during the fire season were obtained for 1995 to 2000. Three years of these data were processed (1996 to 1998; product V_{B1}). The products covering Central and Eastern Russia for 1995 and Eastern Russia for 1999 to 2000 will be the next versions released (V_{B2}). Imagery for a product version to include the region from 28° to 60° E longitude (product V_C) were obtained for 1995 to 1997 but have yet to be processed.

Table 1 summarizes the data used in creating the fire products, the status of the products, and other information on the products, by year and region. Within the Central region and with limited coverage in Eastern Russia (the area covered by the Krasnoyarsk HRPT data), products are complete through 2002, with the intention of continuing mapping fire in the region as long as AVHRR image data are available for fire mapping.

The mapping of fire in European Russia has currently been given a low priority to concentrate on Siberia and the Far East, where fire is largely unmonitored and fewer detection resources are available. Despite the need for consistency, the final products will always be less complete for early years than for recent years because the methods have evolved and improved since the station's installation in 1995. In addition, the SAA archive imagery does not include as many images as are available from a direct download HRPT station (Gutman et al., 2001). Map accuracy, therefore, will vary in space and by year based on data processing improvements and data coverage limitations.

3.2. Fire detection and burned-area mapping methods

The burned-area products were generated using a multi-step process that involved (a) using a contextual active-fire-detection algorithm; (b) creating fire polygons (contiguous areas of fire pixels) from adjoining fire detections; and (c) postfire mapping of burn scars. This procedure was similar to the HANDS method described by Fraser et al. (2000) in that fire detection was used to identify the locations of burned areas. Our algorithm differed in that burn area was defined primarily by aggregating fire detections into fire polygons. To improve the estimate of area burned in large-fire events, burn scars were mapped (i.e., in areas where >50 contiguous fires were detected within a short period). Postfire images alone were analyzed to define burn scars, rather than using both pre- and postfire images, as was done in the HANDS method.

The initial processing of the AVHRR data included calibration in accordance with NOAA-provided prelaunch coefficients for reflectances in spectral bands 1 (0.58–0.68 μm) and 2 (0.725–1.1 μm) and in-flight coefficients for brightness temperatures in bands 3 (3.55–3.93 μm), 4 (10.3–11.3 μm), and 5 (11.5–12.5 μm; Kidwell, 1998). Geo-corrections used the orbital model, initially, and then used a manual georeferencing with ground control points from 1:500,000 scale base maps. Images selected for the creation of burned-area products were processed with these same initial steps.

The active-fire-detection algorithm used in this effort is described in detail by Soja et al. (2004b). Here, we review the algorithm, with additional discussion of the development of the algorithm based on a probabilistic approach that is not presented by Soja et al. (2004b). The algorithm used data from AVHRR spectral bands 2, 3, 4, and 5 from all daytime images. Bands 2 and 5 were used to mask objects that are cool and are highly reflective (e.g., clouds and ice). To avoid potential false detections, water features are also masked using maps of rivers and lakes. Because band 3 is located near the spectral maximum of radiative temperatures that are typical of fire, detection was accomplished using a probabilistic threshold approach based on the spectral response from radiative emissions in band 3. Because band 4 is not sensitive to small objects at temperatures that are typical of fire, the algorithm takes advantage of this difference by only considering pixels where the difference in brightness temperature between the two bands is above a certain threshold.

Table 1
Geographic coverage of products V_A, V_B, and V_C, and summary information on the origin, production, and current status of fire products by year and region. Product V_A is derived from HRPT** data collected at the Krasnoyarsk receiving station; it covers the Central Russia region and part of the Eastern Russia region with limited data. SAA* data has been used for products V_B and V_C to supplement the HRPT data in the eastern and western regions and for early years in the Central region

28E / 60E *Western Russia*	*Central Russia*	120E / 180E *Eastern Russia*
	<---------- Product V_A ----------++++++++++++++++>	
	<---------- Product V_B ---------->	
Year <---------- Product V_C ---------->		
1995	To be processed with SAA* using current methods combined with original HRPT** -based hot spot detections	To be processed with SAA using current methods
1996	To be processed with SAA using current methods	Processed using original HRPT-based hot spot detections & burn scar maps combined with SAA using current methods	Processed using original, but limited, HRPT-based hot spot detections & burn scar maps combined with SAA using current methods
1997			
1998			
1999		Processed using HRPT and current methods	Limited processing using HRPT and current methods complete. Additional SAA images to be processed using current methods
2000			
2001			Processed with limited HRPT coverage and current methods
2002			
2003		Products to be made from AVHRR HRPT & limited MODIS data	Limited HRPT coverage
2004		MODIS-derived products	

Completed
Next priority
Final priority under this program
Not planned under this program
Ongoing production under other programs

* Satellite Active Archive

** High Resolution Picture Transmission

The active-fire-detection algorithm has been developed using the laws of probability as a basis for determining which pixels can be designated as fires. The process of fire mapping submits to probabilistic laws with the probability that a fire is properly recognized as follows:

$P_{\text{fire recognition}}$ is a product of $P_{\text{fire occurrence}}$ and $P_{\text{fire detection}}$

where $P_{\text{fire occurrence}}$ is a product of $P_{\text{fuel ability to ignite}}$ and $P_{\text{occurrence of ignition sources}}$, and where $P_{\text{fire detection}}$ is a function of the radiometer optics parameters: detection ability of the radiance sensor, fire radiance (fire intensity), overpass time, and obscuration by forest crown cover and atmosphere (clouds).

Wildfire occurrence is an irregular process because it depends on weather conditions, which control surface moisture and humidity, and the presence of fire ignition sources. The detection of a target among random noise is a well-known process. The probability of detection has been empirically established as the single-valued function of signal-to-noise ratio (S/N; Lloyd, 1975) that was approximated as (Rosell & Wilson, 1973):

$$P_{\text{fire detection}}(\text{S/N}) \approx 1 - \exp\left\{-0.15[(\text{S/N}) - 1]^2\right\} \quad (1)$$

The S/N depends on the infrared sensor system, atmospheric conditions, forest cover, and wildfire intensity (Hudson, 1969).

We constructed the algorithm for wildfire detection using established infrared detection methods. Using the detected signal, we calculated the probability of fire detection based on brightness temperature. Because the parameters of fires, atmosphere, and forest crown cover were uncertain during detection, we estimated S/N from the temperature field, which is derived from bands 3 of the AVHRR (Dozier, 1981; Matson & Dozier, 1981). In the case of fire detection, the "signal" was the fire radiation energy (temperature of fire derived from band 3) and the "noise" was the variation of the radiant temperature of the background, that is, the surface radiation temperature of the forest cover, steppe, water, clouds, etc. ($T_{\text{background}}$), along the line of image data containing the hot spot (all "nonhot" pixels in the line; Fig. 2). We neglected system noise because it was small in comparison with the background temperature variations.

Fig. 2a shows a sample image with several wildfire burn scars shown as black regions. Brightness temperatures along Line 1 in Fig. 2a reveal three small hot spots and one large area of hot pixels (Fig. 2b). The average temperature of the background along this one line of image data was 29.4 °C, with a standard deviation of 3.7 °C. The computed S/N was 2.92 for the fire 1, 5.46 for fire 2, and 3.84 for fire 3. Using Eq. (1), we calculated a probability of detection of 0.42, 0.95, and 0.70 for these three small fires, respectively. The large region (fire 4) consisted of 11 pixels, with an S/N range of 3.35 to 5.46 for each pixel and a detection probability range of 0.57 to 0.95.

Because AVHRR band 3 saturates at 49.6 °C, we cannot estimate S/N for fires with high intensity. In these cases, by assuming a Gaussian distribution and calculating the mean and standard deviation (σ) of the background temperature in band 3 ($T_{3\text{background}}$), we can assume that objects with T_3 at or greater than 1σ above the $T_{3\text{background}}$ have a 0.68 probability of being fires, based on the probability analysis described above. Pixels at or above $T_{3\text{background}}$ plus 2σ will have a probability of 0.95. The thresholds used in detecting fires, therefore, are determined based on the mean and standard deviation of the background measured along one line of the image and the level of probability desired in fire detection. In practice, we used a probability of 95% ($T_3 \geq T_{3\text{background}}+2\sigma$) to determine if a hot-spot pixel is considered a fire. Therefore, in the example shown in Fig. 2, two of the four detected fires would be classified as fires (fires 2 and 4).

Part of the fire-detection procedure included the creation of a sun glint mask to identify areas of potentially high false detections due to direct solar reflectance. The glint region changed over time, thus, the mask was calculated using a geometry that accounted for satellite viewing angle, local sun angle, latitude, and season. The glint mask formed a strip of high reflectance and high temperature in AVHRR band 3. The length of the glint strip was the Gaussian distribution of the glint intensity, and the width of the glint strip was about 400 km. The glint effect was present primarily for NOAA-14 images in bands 1, 2, and 3. For the other NOAA satellites, this effect was not as significant. After calculating the glint strip location, the area was masked from the image if the strip was on the edge of the satellite pass. Because subsequent satellite passes overlap, the next satellite overpass, which did not contain the glint strip in the area of the previous pass, was used to fill in the fire detections for that area. If the glint strip was in the center of the satellite image, we used the following algorithm: If albedo in band 1 was more than 55% and temperature in band 3 was more than 305 K, but temperature in band 4 was less than 300 K, we assumed that it was sun glint from water or clouds and other high reflecting surfaces. Additionally, because the processing algorithm was implemented manually, decisions were made visually by the interpreter to disregard areas of obvious sun glint. In these cases, a conservative approach was taken, and all doubtful fire detections were dropped.

To summarize, the steps of the fire-detection algorithm are the following:

1. Mask clouds using reflectance in band 2: $\rho_2 < 16\%$,
2. Mask water features using map of rivers and lakes to account for sun glint from water features,
3. Create map of direct reflectance areas (sun glint) to identify the zone of high risk of false detections,
4. Threshold band 3 temperature (T_3): $T_3 \geq T_{3\text{background}}+2\sigma$;
5. Threshold bands 3 and 4 difference: $\Delta T_{3-4} \geq 12$ K; and
6. Mask cool objects (ice) using band 5 temperature: $T_5 \geq 295$ K.

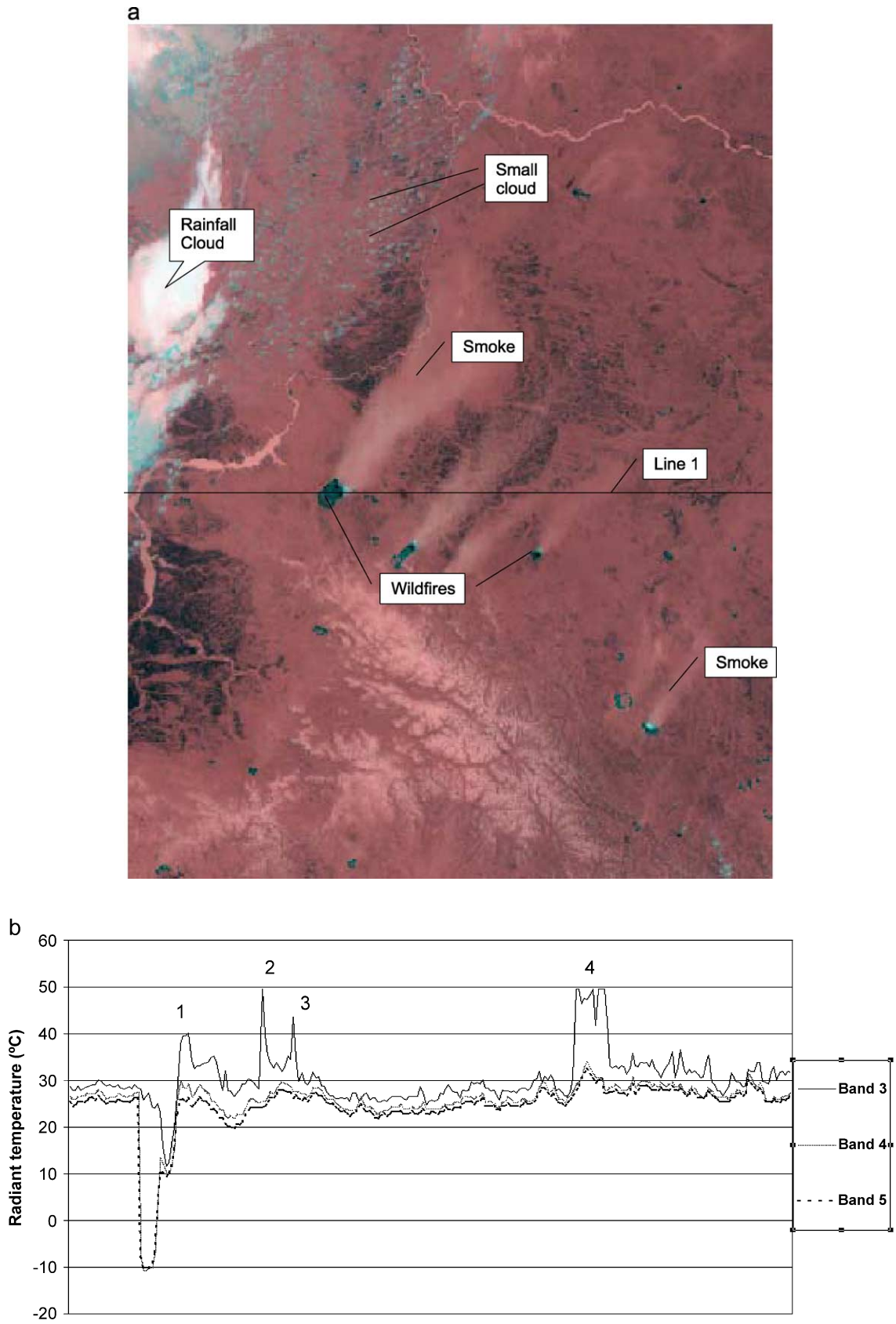

Fig. 2. (a) NOAA 14 AVHRR thermal image showing wildfires near Krasnoyarsk, 25 May 1999 (red=band 3, green=band 4, blue=band 5). (b) Temperature derived from AVHRR bands 3 (3.55–3.93 μm), 4 (10.3–11.3 μm), and 5 (11.5–12.5 μm) across Line 1 (labeled in Panel a) showing four possible fires (marked as 1–4; Soja et al., 2004a,b). (For interpretation of the references to colour in this figure legend, the reader is referred to the web version of this article.)

The fire-detection algorithm described above was used to map the location of probable fires, which were then used to determine the location and size of fires entered into the GIS-based fire database. The area of each fire event was defined using one of two methods: (a) aggregation of detected fire pixels into a fire polygon or (b) postfire burn scar mapping. The fire pixel aggregation method has been modified over the years. Between 1995 and 1998, fire polygons were based on locations determined using the same fire-detection algorithm currently used, but the geographical area of the fire event was artificially defined to represent the area of the burn, rather than using actual fire detections to define burn area, as is now done; the procedure resulted in fire polygons with a block appearance. For the process, as it is currently implemented, which was the process used to map fire polygons from the SAA and local HRPT data from 1999 to the present, fire polygons were created by aggregating groups adjacent and nearby fire pixels (within three to four pixels) detected within a few days of each other, creating more irregular shapes, which more accurately represented the burn area. The coordinates of the center of the aggregated pixel polygon and area of the polygon were then calculated and used in determining the fire's location and size.

In areas where large numbers of fire pixels (>50) were detected within a short period, or in areas where accurate

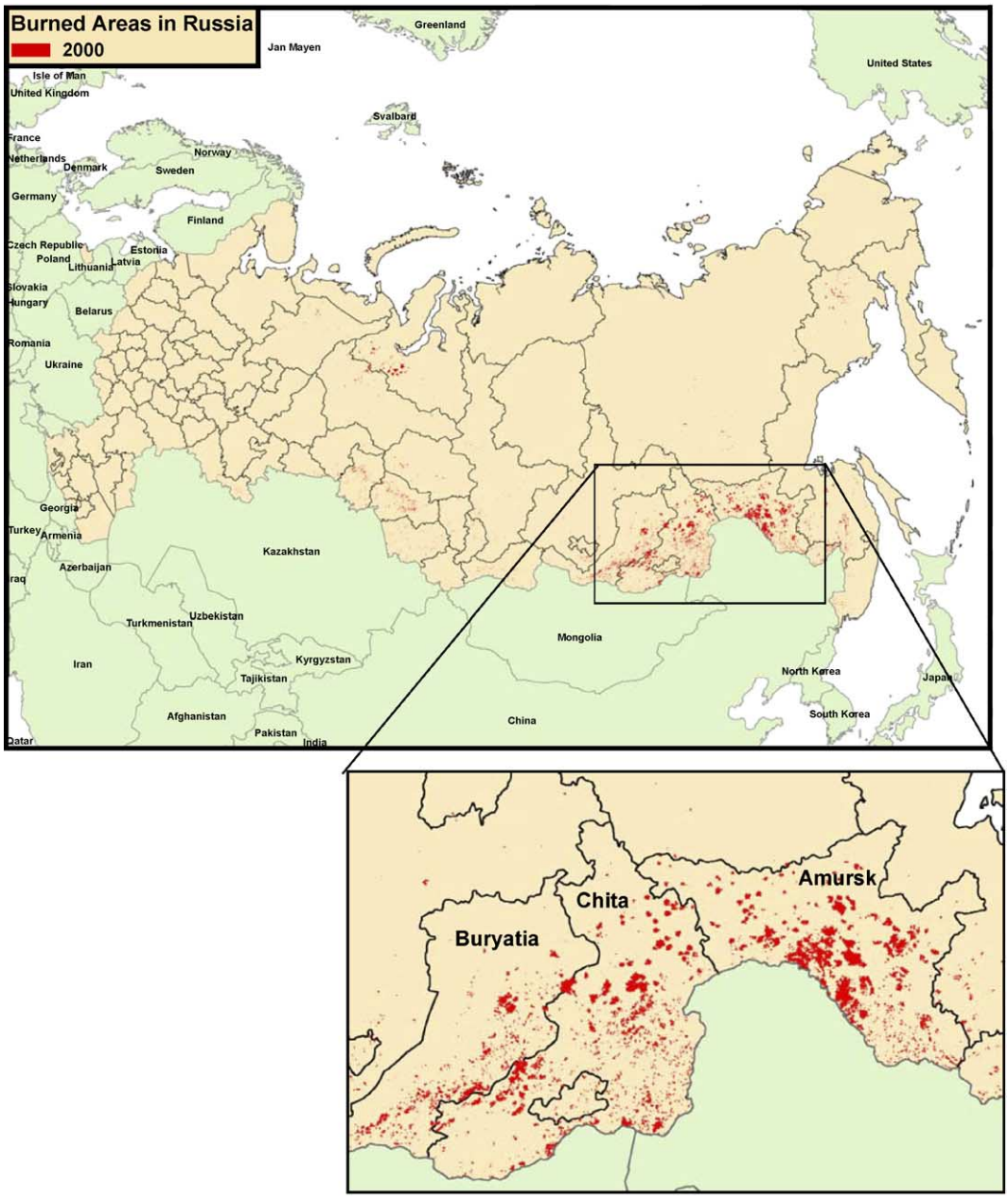

Fig. 3. Example of GIS-based fire product of Russia showing (a) burned area in Russia for 2000 and (b) extensive fire activity detected in the Amur, Chita, and Buryatia regions.

fire boundaries are needed, postfire images were used to map burn scars. This postburn mapping procedure was implemented because it was more accurate than the pixel aggregation method. It could not be implemented at all sites due to lack of cloud-free postfire image data, as well as limitations on available manpower. Where burn scars are mapped, postfire images were georeferenced, then analyzed using standard image analysis tools found in ERDAS. Regions that had been burned were identifiable because band 2 is sensitive to reflectance from green vegetation and substantially decreases following fire events. In several studies, minimum band 2 response (Cahoon et al., 1994) and the difference between bands 1 and 2 have been used to distinguish between healthy green vegetation and burned regions (Fraser et al., 2000; Kasischke & French, 1995; Li et al., 1997). Burn scars are typically warmer than surrounding unburned areas are, thus, the thermal infrared bands were also useful in discriminating burn boundaries. Taking advantage of the unique spectral signal produced in bands 1, 2, and 5 on postfire images, burn scars were outlined using a spectral Euclidian distance (ERDAS, 1999). The image was displayed with band 1 as red, band 2 as green, and band 5 as blue. Using the fire-detection pixel or center of the fire polygon as the starting point, the area was grown based on the spectral characteristics of the pixels adjacent to the pixel known to have burned. Pixels that were adjacent to and spectrally close to the starting point pixel were considered part of the burn scar and added to the polygon. Adjacent pixels were subsequently added to the polygon if spectrally close to the starting pixel until the operator visually determined that the burn area was correctly outlined. Because an unburned pixel had a substantially different spectral signature from a burned pixel, this stopping point was not difficult to determine. The area

Table 2
Example of summary information for 2000 derived from fire databases. The first number column shows the area burned based on aggregated fire detections. The combined values (final columns) use burn scar estimates, where available ("scars"), added to fire-detection-derived area estimates where burn scars were not mapped ("nonscar aggregated fire sites")

Year 2000	Aggregated fire sites from fire detections		Scars		Nonscar aggregated fire sites		Combined	
Region	Area (km^2)	Count	Area (km^2)	Count	Area (km^2)	Count	Area (km^2)	Count
Agin Burat	467.13	84			467.13	84	467.13	84
Altai	1640.06	450			1640.06	450	1640.06	450
Amursk	16,886.84	1144	19,423.07	91	11,620.40	1096	31,043.47	1187
Arkhangelsk	16.22	7			16.22	7	16.22	7
Yevrey	1454.52	155			1454.52	155	1454.52	155
Irkutsk	1245.83	320			1245.83	320	1245.83	320
Kemerovo	335.83	123			335.83	123	335.83	123
Komi-Permackij	9.88	3			9.88	3	9.88	3
Krasnojarsk	1000.20	377			1000.20	377	1000.20	377
Kurgan	95.64	24			95.64	24	95.64	24
Magadan	1481.91	62			1481.91	62	1481.91	62
Neneck	4.72	1			4.72	1	4.72	1
Novosibirsk	3432.06	515			3432.06	515	3432.06	515
Omsk	2193.98	307			2193.98	307	2193.98	307
Orenburg	255.37	19			255.37	19	255.37	19
Primorsk	676.22	112			676.22	112	676.22	112
Altai	42.62	13			42.62	13	42.62	13
Buryatia	8584.72	1210	2600.31	13	7712.88	1196	10,313.20	1209
Komi	695.30	113			695.30	113	695.30	113
Yakutia	983.13	205	55.23	2	965.93	205	1021.16	207
Tuva	947.83	178			947.83	178	947.83	178
Khakasia	242.51	67			242.51	67	242.51	67
Sakhalin							0.00	0
Sverdlovsk	12.93	5			12.93	5	12.93	5
Tamyr	2.37	1			2.37	1	2.37	1
Tomsk	850.49	193			850.49	193	850.49	193
Tumen	278.65	75			278.65	75	278.65	75
Ust-Ordynsk Burat	265.52	76			265.52	76	265.52	76
Khabarovsk	3616.90	286			3616.90	286	3616.90	286
Khanty-Mansysk	1021.77	196	69.38	2	1013.11	195	1082.49	197
Chelyabinsk	19.12	7			19.12	7	19.12	7
Chita	19,272.77	1756	13,024.64	66	14,771.35	1720	27,795.99	1786
Chukotia	31.41	1			31.41	1	31.41	1
Evenk	17.49	8			17.49	8	17.49	8
Yamalia-Nenetsia	2439.57	206	2915.98	30	1559.75	201	4475.74	231
Russia	70,521.52	8299	38,088.63	204	58,976.15	8195	97,064.78	8399
Non-Russia	23,924.93	2448	37,341.70	47	21,078.23	2400	58,419.93	2447

classified as burn scar in this method was outlined in ERDAS and converted to a GIS polygon feature.

3.3. Product accuracy assessment methodology

As an initial evaluation of the products, a local scale evaluation of the hot spot and burned-area products has been performed from 2001 and 2002 over north-central Russia (in or near Yakutia) using Landsat ETM+ imagery. Burned-area estimates from the AVHRR burn scar product (2001 only; not available in 2002) and from the aggregated AVHRR fire-detection products (2001 and 2002) were compared with burned-area estimates from ETM+. These estimates were derived through the manual delineation (digitizing) of apparent burn scars in single images at the scale of 1:100,000. The approximate dates of burning of each scar on the ETM+ imagery were determined by active-fire observations from the MODIS Land Rapid Response System (Justice et al., 2002) to minimize misinterpretation of burn scars from previous years and to ensure that the absence of burning occurred between the date of the ETM+ acquisition data and the AVHRR burn scar mapping. Inventory analyses were performed from individual scars and from total area estimates within each ETM+ image, but no spatial coincidences were calculated. Vegetation cover types within the ETM+-derived burned areas were determined from the University of Maryland 1-km AVHRR Land Cover Classification data set (Hansen et al., 2000).

A more extensive evaluation of the AVHRR burned-area products is currently being carried out using ETM+ data from 1999 through 2002 from additional regions of Russia and will be reported in a forthcoming article (Hewson et al., in preparation).

3.4. Analyses of the spatial distribution of fire

To analyze the spatial distribution of fire in the region, we used two data sets that were available in a GIS format and, therefore, could be easily merged with the burned-area databases created during this study. The first data set consisted of the seven land-cover categories defined by Stolbovoi and McCallum (2002): cropland, pasture, forest, bogs, swamps, grasslands and shrubs, and bare land. This database was available from the International Institute for Applies Systems Analysis (IIASA; http://www.iiasa.ac.at/Research/FOR/russia_cd/lcov_des.htm). The second data set, developed by Kurnaev (1990), divides the country into 10 broad vegetation zones along latitudinal and longitudinal gradients. The 10 zones include (from north to south) arctic desert, tundra, forest tundra, meadow and meadow-forest, taiga, mixed forests, forest steppe, steppe, semidesert, and desert. This data set was obtained from the United Nations Environment Programme (UNEP; http://www.grida.no/prog/polar/ecoreg/dsi/kurnaev_sample_e.html).

4. Results

4.1. Fire database description

The GIS database created under this project includes daily hot spot locations and attributes for all detected fires. Also included are databases of fire polygons derived from the daily data and burn scar polygons for each year (Fig. 3). Each hot spot detection in the daily data file includes the following attributes: latitude, longitude, area, date, time, satellite number, administrative division, region, nearest town, and

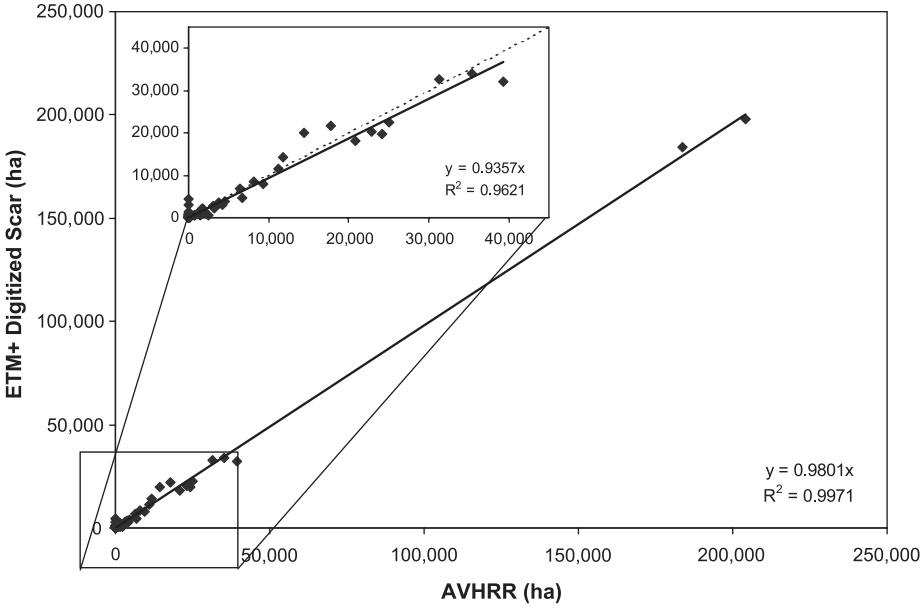

Fig. 4. Comparison of burned area from 60 fires in 2001 estimated from AVHRR product and Landsat ETM+ digitized area. The analysis shows good agreement between AVHRR estimates and ETM+ estimates even when the two larger fires are not included.

Table 3
Three predominant vegetation cover types within area burned in Landsat ETM+ scenes (%)

Landsat ETM+ scene (WRS-2 path row and date)	Evergreen needleleaf forest	Deciduous needleleaf forest	Mixed forest	Woodland	Wooded grassland	Grassland
120_013 2001 Aug 2				19.7	61	7.4
122_015 2001 Aug 16		16.2		56.2	22.3	
123_016 2001 Aug 23		25.4		57.3	15.5	
125_015 2001 Sep 6		6.4		71.9	12.5	
132_018 2001 Aug 22	49.2	24.9	19.9			
122_016 2002 Jun 16		9.8		59.3	28	
122_016 2002 Aug 3		16.2		54.4	26	
125_016 2002 Jul 23		15.4		73.4	10.1	
125_017 2002 Jul 7		31.4		55.9	4.5	
125_017 2002 Jul 23		18.3		68.9	5.6	

distance and heading to nearest town. Each polygon in the yearly files contains the following attributes: date of first detection, date of last detection, latitude and longitude of the polygon center, area of the polygon, forest name, region name, nearest town, and distance and azimuth to the nearest town. Fire scar polygon databases contain the following: latitude and longitude of the polygon center, area and perimeter of the polygon, date of image analysis, year of fire, and region name. Yearly summary reports are also produced with similar information content (Table 2). Currently, maps of fire in the Central region are complete, as are 3 years of maps covering the Eastern region.

Fire polygons and mapped burn scars are both held as ArcView GIS shape files, a GIS database format. To produce the final burned-area maps (such as Fig. 3), the two data sets are combined. When area-burned statistics and information products were created, the area estimated from the aggregation of fire detections were discarded in favor of the more reliable burn scar map estimate of area. Because the fire data are held in GIS database format, it is possible to derive a variety of fire statistics, to analyze seasonal fire patterns, and to visualize wildfire geographic distribution within the region.

All products are available for download at http://www.glcf.umiacs.umd.edu/data/russiaforest/. During the fire season, the daily data files and summary reports are available directly from the Krasnoyarsk station's file transfer protocol (ftp) site: ftp://friend.getdata@195.161.57.194/Dailydata/.

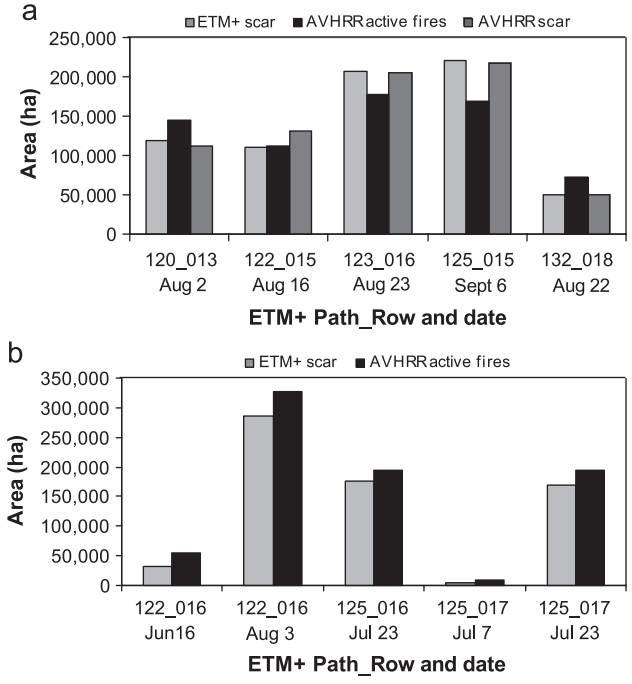

Fig. 5. (a) Comparison of burned area estimates acquired from Landsat ETM+, the AVHRR active-fire-detection product, and the AVHRR burn scar product in five ETM+ images in 2001; and (b) comparison of burned area estimates acquired from Landsat ETM+ and the AVHRR active-fire-detection product in six ETM+ images in 2002.

Table 4
Comparison of estimated annual area burned (km^2) from this study, the Russian Federal Forest Service records, and other remote-sensing-based studies for single years

Year	This study	Russian Federal Forest Service[a]	Soja et al. (2004)[b]	Single-year studies (see notes)
1996	60,466	23,120	22,700; 24,400	
1997	15,405	9,840	11,400; 11,400	
1998	114,914	53,400	36,900; 95,300	110,000[c]; 133,000[d]
1999	54,338	10,480	51,400; 54,400	
2000	97,065	16,400	70,500; 97,100	121,245[e]; 200,000[f]
2001	75,600	12,294		
2002	121,419	18,340		
Annual average	77,030	18,181		

[a] Shvidenko and Goldammer (2001) and Davidenko (personal communication).

[b] Estimates based on an earlier version of the products without added SAA data analyses. The first number shows the analysis using hot spots only, the second number is hot spots plus mapped burn scars.

[c] For eastern Russia and part of Mongolia (Kajii et al., 2002).

[d] Includes adjustments for areas not sampled and undetected fires (Conard et al., 2002).

[e] Fire area in vegetation types of all of Russia not including grasslands and croplands extracted from GBA2000 database (http://www.gvm.jrc.it/fire/gba2000/index.htm; Grégoire et al., 2003).

[f] Estimated from burn scars as detected by ATSR-2 under GLOBSCAR (Simon et al., 2004).

4.2. Product accuracy assessment results

The accuracy assessment carried out for this study includes 60 different fire events. The individual AVHRR-derived burned areas showed good agreement with the ETM+ estimates (Fig. 4). Twenty-four of the smaller fires, most <1000 ha, that were mapped in the ETM+ images were not mapped by AVHRR. Of the fires that were mapped, most fire areas were similarly estimated by both sensors, although the AVHRR method most often overestimated area as compared with ETM+.

In the selected ETM+ scenes, the predominant vegetation type to burn was woodland (as determined from the AVHRR Global Land Cover Classification; Hansen et al., 2000), with the exception of scenes 120_013 (wooded grassland in both 2001 and 2002) and 132_018 (evergreen needleleaf forest; Table 3). This is consistent with the analysis described below, which shows that most burned area is forest type with some grassland and shrubland burning.

The comparison of total area mapped within the ETM+ scenes shows that, regardless of the predominant vegetation type burned, the estimates of the AVHRR burn scar mapping method were in good agreement with those from the ETM+ (Fig. 5a). The aggregated AVHRR hot spot method provided less consistent burned-area estimates, indicating the stronger dependence of this product on the spatiotemporal sampling of active fires by AVHRR. An analysis of AVHRR active fires for 2002 also showed a tendency to overestimate the area burned by 10% (Fig. 5b).

Although not comprehensive, this analysis indicates that, at select sites, the AVHRR-derived fire area is a good estimate of actual area burned. The results are encouraging that the fire database provides accurate area burned information where fires are mapped.

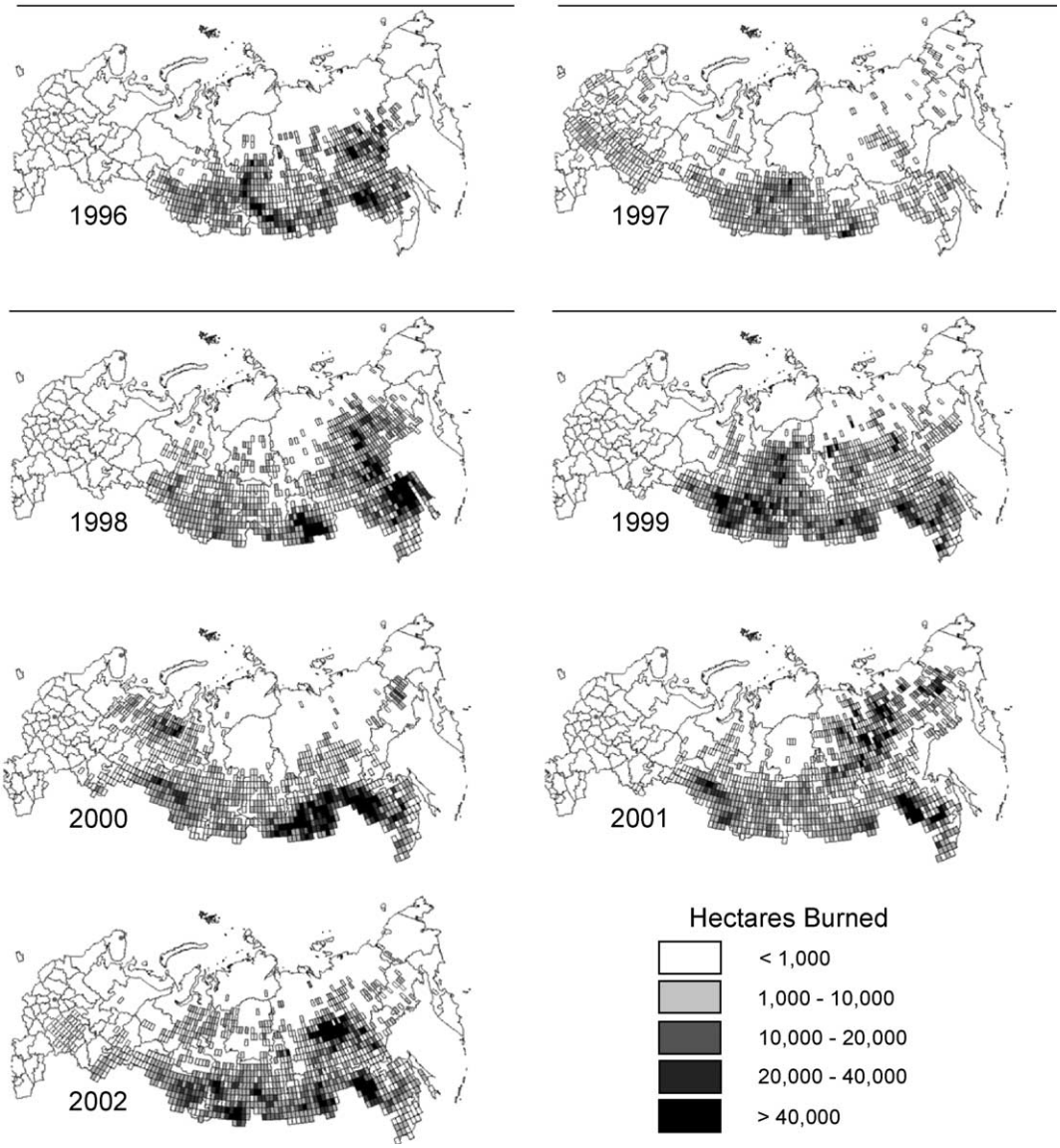

Fig. 6. Annual area burned for 1996 to 2002 mapped to a 1°×1° grid for use in regional-scale emissions modeling.

4.3. Spatial and temporal distribution of fires in Eastern Russia

An analysis of the fire products showed that, during the period 1996–2002, an average of 7.7×10^6 ha (77,000 km^2) yr^{-1} of fire occurred in Russia (Table 4). There was almost an order of magnitude of interannual variability in area burned (1.5×10^6 ha in 1997 to 12.1×10^6 ha in 2002). The variability observed in area burned from year to year in this data set was similar to that observed in the North American boreal forest region (French et al., 2002). The burned-area estimates generated from the AVHRR observations is 4.2 times the average area burned reported by the Russian Federal Forest Service for the entire country (although the Federal Forest Service monitors fire only in a limited region, as described in the Background section), with the ratio for individual years ranging from 1.6 to 6.6 (Table 4). A statistical correlation between the reported burned areas and AVHRR estimates indicates that the official statistics are not an unbiased sample of fire activity (R^2=0.32, p<0.19). Finally, the burned-area estimates using a combination of active-fire detection and burn scar mapping were 15% higher than those produced from analyses of active-fire detections alone (e.g., the Soja et al., 2004b, data in Table 4).

Fire activity was not evenly distributed throughout Russia, with the location of fires variable by year (Fig. 6). Over the study period, three regions experienced 85% of the area burned: (a) the Far Eastern region, consisting of Yakutiya and the Khabarovskiy kray (36%), (b) the area just north of the Chinese border, consisting of the Amurskaya and Chitinskaya Oblasts and the Republic of Buryatiya (33%), (c) and South Central Siberia, consisting of the Krasnoyarskiy Kray, the Irkutskaya and Novosibirskaya Oblasts, and the Republic of Tyva (16%).

As expected, the most common land cover type where for fire occurrence was forest, where 55% of the total area burned occurred (Table 5). The crops and pastures, swamps and bogs, and grass and shrubs land-cover categories experienced 13% to 15% each. The distribution of burned area between different land-cover types is important for not only estimating the damage from fires to important natural resources, such as productive forest land, but also in estimating emissions from Russia fires. In particular, the burning of forests, as well as bogs and swamps, common in the boreal region, can lead to much higher emissions than the will the burning of other land-cover types. Thus, interannual variations in carbon emissions from fires are not only dependent on differences in area burned, but also on the quantity and quality of fuels available for burning (see, e.g., Kasischke et al., in review; Soja et al., 2004a).

The distribution of area burned in the different forest region categories of Kurnaev (1990) in Table 5 shows that, on average, 65% of the area burned occurred in the taiga zone, 20% in the steppe and forest steppe zones, 12% in the mixed forest zone, and 3% in the tundra and forest-tundra zones, and is indicative of the latitudinal gradient that exists in fire activity. This gradient is also present within the taiga

Table 5
Fraction of total area burned by land-cover type or forest vegetation zone. A breakdown of fraction burned within the coniferous forest subzones is also shown. Sources for the land cover and forest zone data sets are given in the notes

	Year							
	1996	1997	1998	1999	2000	2001	2002	All years
Landcover type[a]	*Fraction of total area burned*							
Croplands and pasture	0.095	0.242	0.118	0.249	0.144	0.123	0.152	0.149
Forest	0.659	0.504	0.601	0.459	0.526	0.458	0.616	0.554
Bogs and swamps	0.106	0.044	0.086	0.115	0.192	0.227	0.114	0.137
Grass and shrubs	0.127	0.147	0.164	0.153	0.104	0.170	0.094	0.134
Bare and not classed	0.013	0.063	0.030	0.023	0.033	0.022	0.023	0.026
Forest zone[b]								
Tundra	0.018	0.021	0.037	0.017	0.033	0.044	0.012	0.027
Forest-tundra	0.000	0.001	0.000	0.000	0.001	0.002	0.001	0.001
Taiga*	0.747	0.585	0.773	0.541	0.583	0.564	0.695	0.652
Mixed forests	0.125	0.077	0.039	0.124	0.160	0.223	0.096	0.122
Forest-steppe	0.086	0.235	0.101	0.255	0.173	0.134	0.127	0.147
Steppe	0.021	0.075	0.049	0.057	0.048	0.031	0.065	0.048
**Taiga subzones*[b]	*Fraction of taiga area burned (see above)*							
Open taiga	0.052	0.014	0.046	0.050	0.068	0.296	0.016	0.077
North taiga	0.021	0.049	0.032	0.062	0.062	0.146	0.025	0.053
Middle taiga	0.421	0.183	0.616	0.449	0.431	0.206	0.393	0.428
South taiga	0.506	0.754	0.306	0.439	0.439	0.352	0.566	0.442

[a] Classes grouped from 7 land cover type classes from International Institute for Applies Systems Analysis (IIASA) web site http://www.iiasa.ac.at/Research/FOR/russia_cd/lcov_des.htm (Stolbovoi & McCallum, 2002).

[b] Forest zones are from United Nations Environment Programme (UNEP) web site http://www.grida.no/prog/polar/ecoreg/dsi/kurnaev_sample_e.html (Kurnaev, 1990).

zone, where 13% of the fire activity occurs in the open and northern taiga, 43% in the middle taiga, and 44% in the southern taiga. There is year-to-year variation in the distribution of fire in different forest zones. For example, in 2001, 44% of the area burned in the taiga zone occurred in open and northern taiga zones.

Finally, our analysis of the temporal characteristics of the fire products shows that the fire season in Russia tends to be longer than in the North American boreal forest, beginning in mid-April and extending into early October (Fig. 7). The fire season in the North American boreal forest region begins in early May and ends in mid-September (Kasischke et al., 2002). While fires in Russia begin as early as March and burn as late as October, 93% of all fire activity occurred between April and September for the 1996–2002 period, and 55% of the total annual burning took place prior to the beginning of July. As with annual statistics, burning varied considerably from month to month (Fig. 7a). However, monthly burning tends to follow specific patterns based on the total annual area burned. For example, fire activity during the low-fire years of 1996, 1997, and 1999 occurs early in the fire season, with 70% of the area burned occurring before July (Fig. 7b). In contrast, during the large-fire years of 1998 and 2002, there is a shift towards late-season fires, with 56% of the burned area occurring at the beginning of July. In these two large-fire years, the majority of burning for the year occurred during the month of August, while burning in August was relatively low in other years, particularly the years of low total area burned.

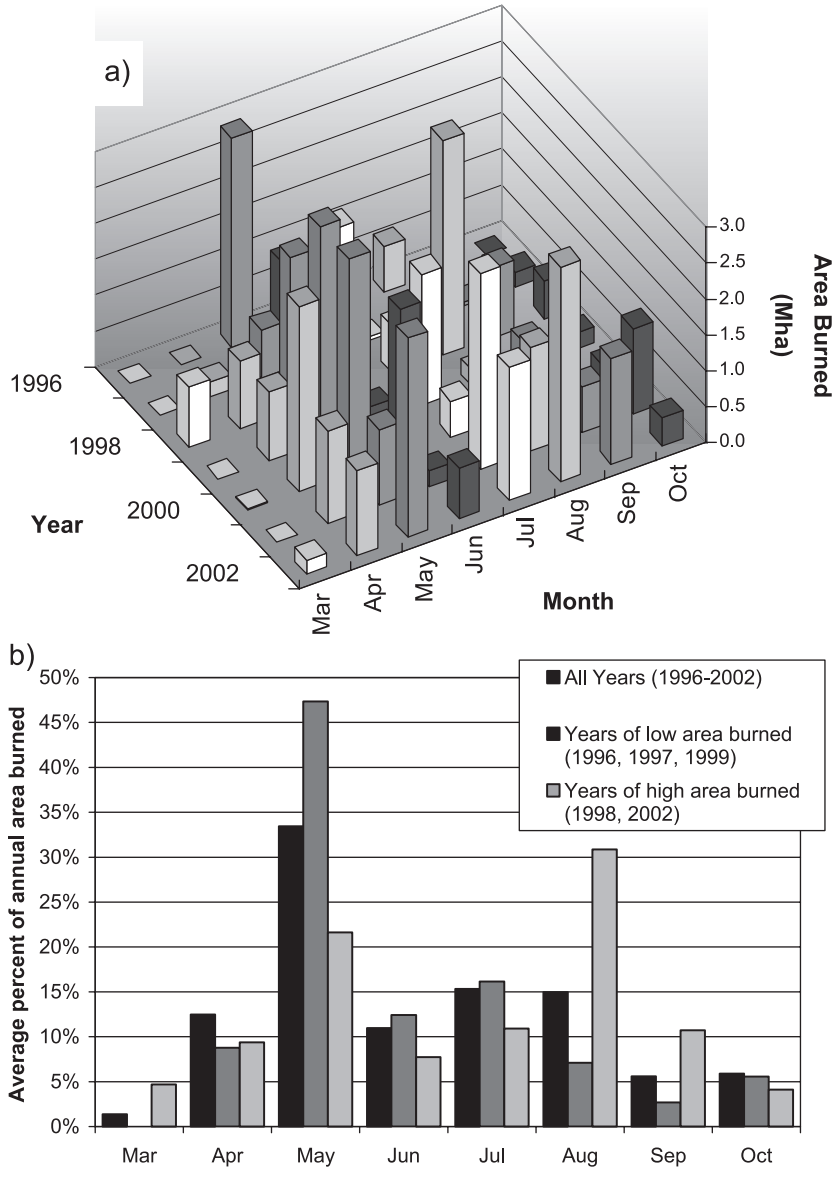

Fig. 7. (a) Area burned in Russia by month and year showing large inter- and intra-annual variability. (b) Percent of annual area burned by month for an average of all years, 3 years of low fire activity, and 2 years of high fire activity. In low years, burning is more often in the early part of the season, while fire activity shifts to later in the season in large-fire years.

5. Discussion and product limitations

The burned-area products for eastern Russia presented in this paper have a broad range of applications. One of the salient features of this data set is that the information is both spatially and temporally resolved, providing a wealth of information to managers and scientists trying to better understand the patterns of fire that occur in this region. Fire managers are currently using the daily hot spot detection product to help monitor and manage fire-suppression activities. Climate change and carbon cycle scientists will find the data helpful in defining the general fire regime, including the amount of area burned, the seasonality of fire, and the spatial patterns at daily, monthly, and annual time scales. GIS-based data on fires such as these can be used in conjunction with other geospatial data products to calculate and model the influences of fire on the landscape and atmosphere, including estimating emissions of carbon-based greenhouse gases from fire (see, e.g., French et al., 2000, 2002; Kasischke & Bruhwiler, 2002; Kasischke et al., in review; Soja et al., 2004a), and the effects of fire on vegetation cover (Hicke et al., 2003). Recent research using these data shows that interannual variations in fire in boreal regions are an important factor in regulating variations in atmospheric trace gasses (Kasischke et al., in review; Van der Werf et al., 2004). Previous studies have shown that AVHRR image data are particularly useful in defining burned areas at a regional scale or in remote regions where the ability to monitor fire is difficult and cost prohibitive (Cahoon et al., 1994; Fraser et al., 2000; Kasischke & French, 1995; Justice et al., 1996; Li et al., 1997). However, the frequency of satellite overpass and persistent cloud cover in boreal regions limits the ability of the instrument to detect all active fires (Boles & Verbyla, 2000; Flannigan & Vonder Haar, 1986; Kasischke et al., 2002). The number of satellite overpasses east of the Urals were typically four to eight per day, resulting in many hours of unmonitored fire activity. In addition to limited imaging times, thick cloud cover is persistent in Siberia during the summer fire season, often covering greater than 60% of the region (Warren et al., 1986), creating more obstacles to fire monitoring. These confounding factors make fire detection a probabilistic process, requiring a detection method that takes these factors into account, as is described above. Fire detection has been shown to be useful for defining patterns of fire (Cahoon et al., 1992; Justice et al., 1996; Olson et al., 1999; Soja et al., 2004b). However, used on its own, it only provides a snapshot of the area burned and is therefore limited for estimating area burned, particularly in boreal regions, where most area is burned in large fires (Stocks, 1991; Valendik, 1996). Li et al. (2000) found that fire detection underestimated area burned in boreal Canada by 31% in 1995 and 37% in 1994. Conversely, overestimates from fire detection are possible from reflective surfaces and small fires (<1 km^2) that saturate band 3 (Dowty, 1993). Soja et al. (2004b) found that active-fire detection alone, compared with the combined result of fire detection and burn scar mapping, underestimated area burned in this region by 7% in 1996, 61% in 1998, 5% in 1999, and 27% in 2000. The larger differences in 1998 and 2000 are the direct result of a greater number of large fires, thus, it is possible that estimates of burn area made from fire detections is more representative in less-active-fire years. The burned-area products presented in this paper combine fire detection and burn scar mapping to take advantage of the benefits of each of these techniques and to limit the disadvantages.

As described in this paper, the estimate of burn area was accomplished in two ways: first, fire-detection pixel aggregation, where detected fire pixels are aggregated into a fire polygon, and second, postfire burn scar mapping, where burn area is mapped from the postfire scar. It is recognized that fire pixel aggregation is not an optimal method for mapping burn area, but we consider it more accurate than is assuming that burn area is limited to only pixels detected at the time of satellite overpass. Furthermore, in some instances, fires detected as hot spots do not leave recognizable scars, and in these cases, burned area cannot be estimated without the pixel aggregation step. In an effort to improve the estimate of burn area, burn scars were mapped in regions of significant fire activity. Implementation of the additional step of burn scar mapping ensures that larger fires are adequately quantified, and proper mapping of large fires provides a fairly accurate estimate of total area burned, since the majority of burning occurs in large fires (Stocks, 1991). The two methods for fire-area estimation, which were both based on the identification of fires through the probabilistic fire-detection algorithm, are combined with each other to produce the area-burned products presented in this paper.

We consider our estimates of area burned in Russia to be conservative because of the processing and data limitations described above and because of the nature of fire detection from space. Small fires can be missed because the energy given off is too low to be detected. In addition, it is probable that some fires will not be detected due to the limited number of satellite overpasses and because cloud cover often obscures fire detection in this region. Furthermore, postfire burned-area mapping was done in limited locations due to resource and time limitations, resulting in a possible underestimation of area. However, because most of the area burned in boreal regions is consumed by large fires (Kasischke et al., 2002; Stocks, 1991; Valendik, 1996), and this process emphasizes accurate mapping of larger fires, we are confident that our products adequately capture the spatial and temporal extent of wildfire burning in Siberia for the years studied.

A close inspection of GIS-based maps shows that fire polygons created from early analyses may not be as accurate

as the latter products are, a result of refinements in the procedures used to define fire size from the hot spot data. Despite this and previously discussed shortcomings, the products presented here are more comprehensive in both spatial coverage and number of years covered when compared with other fire maps and products in the region. Furthermore, although the products have yet to be systematically validated, the methodology used in generating these products has been shown to remove false fire detections (commission errors) adequately (Li et al., 2000). Commission error is a critical problem if the data are to be used for identifying fire locations for limited scale studies or for assessing fire activity in a relative sense (e.g., from month to month or region to region; Kasischke et al., 2003).

Others have mapped fire in northern Asia, but none as extensively as this project (Table 4). Kajii et al. (2002) mapped fire in Siberia and the Far East for 1998 using a threshold-based detection algorithm checked by regional experts. Their estimated area burned for the region was 110,000 km^2, which is similar to the estimates found from our products, although no direct comparison has been made of the two products to determine if they geographically agree. For the Global Burnt Area-2000 (GBA2000) project (Grégoire et al., 2003; Tansey et al., 2004), the total area burned in the forests and woodlands of Russia (not including grasslands and croplands, which are primarily found in Western Russia) is estimated to be more than that mapped in our products for 2000. Similarly, results of the GLOBSCAR program, which maps fire scars using the ATSR-2 sensor (Simon et al., 2004), estimate more area burned than this study did in 2000. As with the Kajii et al. (2002) study, no geographic comparison of the GBA-2000 or GLOBSCAR products has been made. Soja et al. (2004a) generally estimated less area burned in an analysis of an earlier version of this product using hot spot detections alone. Estimates between this study and that of Soja et al. (2004a) are closer when burn area maps are added to the area estimated with only fire detections, particularly in 1999 and 2000, because limited additional SAA-based analyses are complete for the recent analysis.

Under this fire mapping project, we devised a staged program to improve the temporal and geographic extent of fire maps for Russia. The strategy has been to use existing and ongoing fire monitoring and mapping activities occurring at the Sukachev Forest Institute using the AVHRR HRPT image data (product V_{A1}). To improve on this product, we have acquired additional image data from the SAA. The additional images increase the geographic extent of the fire products and improve maps for early years when burned-area products were not as rigorously produced as they are currently (product V_{B1}). The result of this mapping effort will be a set of daily and yearly databases of detected and mapped fires for all of Russia from 1995 to 1998 and most of the area east of the Ural Mountains from 1995 to 2002. Complete coverage of Eastern Russia will be limited for the years 2001 and 2002 because data from outside of the Krasnoyarsk HRPT acquisition area (SAA data) will not be obtained and processed for these years, as planned for years 1995 to 2000, due to project resource limitations.

As reported, an initial evaluation of the AVHRR-derived products using ETM+ imagery has shown good agreement with Landsat-based estimates of burn area for a small set of fires. We are now in the process of performing a comprehensive accuracy assessment of the fire products using a larger validation data set produced from Landsat ETM+ imagery, covering a wider range of forest and vegetation cover types in Russia than done in the initial evaluation. The analysis will include both inventory and geospatial validation. We plan to report accuracy figures both for the hot spot detection and the burn scar products, as well as the combined hot spot/burn scar product. This will enable the assessment of the products for detecting both the number of fires and their areal extent. We will be determining the accuracy of the fire products, including overall accuracy and area regression analyses, using a set of over 30 ETM+ scenes sampled across the full spatial extent of the AVHRR fire products. The results of the accuracy assessment will be reported in a separate publication currently in preparation (Hewson et al., in preparation).

The production of GIS-based wildfire maps is planned to continue for the region around Krasnoyarsk. A MODIS ground station has recently been installed at the Sukachev Forest Institute to replace the AVHRR HRPT data for fire monitoring and other broad-scale remote-sensing applications. The MODIS system is well designed to provide data for the detection and mapping of fire events (Justice et al., 2002). The coverage area for the station will not be as extensive as the AVHRR coverage region; it will cover from approximately 65° to 110° E longitude and 45° to 65° N latitude. The MODIS active-fire products will be generated with the assistance of NASA within the standard MODIS production system, as well as within the MODIS Land Rapid Response System. The MODIS burned-area products (Roy et al., 2002) are currently being evaluated over various regions of the globe, including Russia. Global operational generation of the burned-area products is planned to begin within the next year.

As the observing systems transition from AVHRR to MODIS and then to the future operational VIIRS (Visible and Infrared Radiometer Suite) sensors, continuity of the fire products needs to be ensured. Fire mapping and monitoring activities in Russia are currently being organized into a regional network within the GOFC/GOLD program, including the Sukhachev Forest Institute in Krasnoyarsk. GOFC/GOLD promotes the continuous generation of high-quality fire products, their validation based on standard protocols, and their efficient distribution to various user communities. The validation of new products is essential and is required under the guidelines of the GOFC/GOLD program. The AVHRR-based fire mapping and monitoring efforts discussed in this paper represent an integral part and a major contribution to this endeavor. The network has a

partnership with the MODIS Fire Team, which currently provides active-fire information from the Rapid Response System. In the future, MODIS data from the Krasnoyarsk station and several other Russian direct broadcast receiving stations will be incorporated into an integrated regional observing system (Loupian et al., in press).

6. Summary

The data set presented in this paper contains information on fire occurrence and location in the boreal forest region of Russia, from 1996 to 2002. The methodology for producing these maps uses AVHRR HRPT imagery from a collection station in Krasnoyarsk and additional archived imagery provided from the SAA. Both daily hot spots and fire polygons are created in this process. The products extensively cover the area east of the Ural mountains and will have some limited information on fire in Western Russia. The products are the most spatially and temporally comprehensive data of area burned compiled for Russia that is currently known to the authors. Daily hot spot locations, as well as aggregated yearly products, are available for the 9 years. Fire mapping is expected to continue over the next few years at the Krasnoyarsk receiving station using AVHRR and MODIS.

Overall, we consider the burn area mapped with these products to be a conservative estimate of actual area burned for several reasons: Fire cannot be detected through cloud cover, leaving fires undetected; satellite overpasses limit the detections to fire active at selected times in the day; and only large burn scars are rigorously mapped. However, the products represent a good record of known fire events, compares well with other existing information and initial data comparisons, and are currently in the process of being systematically validated. Through the validation process, we will be able to define the accuracy of the area estimates and calculate a bias to be used in modeling fire in Russia.

Analyses of earlier remote-sensing-based fire products of Russia have shown that fire is poorly documented and fire regime is not well known, especially in Central and Eastern Russia. We expect that the new products generated under our project will be helpful for an accurate understanding of the spatial and temporal patterns of fire in the Russian boreal forest. In our initial analyses, we have looked at both spatial and temporal patterns of fire. Most fire occurs in forested types, some with substantial areas of wetlands, an important consideration for carbon emission studies. The seasonality of fire occurrence is related to the total area burned in the year, as has been observed in North American boreal regions. Furthermore, as expected, the data products show that fire is both inter- and intra-annually variable, making it important to use more than 1 year of data to assess the full impact of fire.

Acknowledgements

The research presented in this paper was supported, in part, by NASA grant NAG59440 to the University of Maryland and Altarum Institute (formerly ERIM). We would also like to acknowledge the technical and financial support by NASA Headquarters, the Russian Fundamental Investigation Foundation (Grant 00-05-72048), and U.S. Civilian Research and Development Foundation (RB1-2416-KY-002). I. Csiszar and T. Loboda were supported, in part, by the NASA New Investigator in Earth Science (NAG512667) and Land Cover Land Use Change (NNG04GC82G) Programs. The authors would like to acknowledge the help of the anonymous reviewers and Mr. Peter Schlesinger for their detailed comments on earlier drafts.

References

Ahern, F. J., Goldammer, J. G., & Justice, C. O. (2001). *Global and regional vegetation monitoring from space*. The Hague, The Netherlands: SPB Academic Publishing.

Amiro, B. D., Todd, J. B., Wotton, B. M., Logan, K. A., Flannigan, M. D., Stocks, B. J., et al. (2001). Direct carbon emissions from Canadian forest fires, 1959–1999. *Canadian Journal of Forest Research*, *31*, 512–525.

Apps, M. J., Kurz, W. A., Luxmoore, R. J., Nilsson, L. O., Sedjo, R. A., Schmidt, R., et al. (1993). Boreal forests and tundra. *Water, Air and Soil Pollution*, *70*, 39–53.

Arino, O., Simon, N., Piccolini, P., & Rosaz, J. M. (2001). The ERS-2 ATSR-2 World Fire Atlas and the ERS-2 ATRS-2 World Burnt Surface ATLAS projects. Proc. 8th ISPRS Conference on Physical Measurements and Signatures in Remote Sensing, AUSSOIS, 8–12 Jan 2001.

Barbosa, P. M., Gregoire, J. -M., & Pereira, J. M. C. (1999). An algorithm for extracting burned areas from time series of AVHRR GAC data applied at a continental scale. *Remote Sensing of Environment*, *69*, 253–263.

Boles, S. H., & Verbyla, D. L. (2000). Comparison of three AVHRR-based fire detection algorithms for interior Alaska. *Remote Sensing of Environment*, *72*, 1–16.

Cahoon Jr., D. R., Levine, J. L., Cofer III, W. R., & Stocks, B. J. (1994). The extent of burning in African savannas. *Advances in Space Research*, *14*, 447–454.

Cahoon Jr., D. R., Stocks, B. J., Alexander, M. E., Baum, B. A., & Goldammer, J. G. (2000). Wildland fire detection from space: Theory and application. In J. L. Innes, M. Beniston, & M. M. Verstraete (Eds.), *Biomass burning and its inter-relationship with the climate system* (pp. 151–169). Dordrecht: Kluwer Academic Publishers.

Cahoon Jr., D. R., Stocks, B. J., Levine, J. S., Cofer III, W. R., & Barber, J. A. (1996). Monitoring the 1992 forest fires in the boreal ecosystem using NOAA AVHRR satellite imagery. In J. S. Levine (Ed.), *Biomass Burning and Global Change* (pp. 795–801). Cambridge, Mass.: MIT Press.

Cahoon Jr., D. R., Stocks, B. J., Levine, J. S., Cofer III, W. R., & Chung, C. C. (1992). Evaluation of a technique for satellite-derived area estimation of forest fires. *Journal of Geophysical Research*, *97*, 3805–3814.

Conard, S. G., & Ivanova, G. A. (1997). Wildfire in Russian boreal forests—Potential impacts of fire regime characteristics on emissions and global carbon balance estimates. *Environmental Pollution*, *98*, 305–313.

Conard, S. G., Sukhinin, A. I., Stocks, B. J., Cahoon, D. R., Davidenko, E. P., & Ivanova, G. A. (2002). Determining effects of area burned and fire

severity on carbon cycling and emissions in Siberia. *Climatic Change*, *55*, 197–211.

Csiszar, I., Abdelgadir, A., Li, Z., Jin, J., Fraser, R., & Hao, W. -M. (2003). Interannual changes of active fire detectability in North America from long-term records of the advanced very high resolution radiometer. *Journal of Geophysical Research*, *108*, 4075.

Csiszar, I., & Sullivan, J. (2002). Recalculated pre-launch saturation temperatures of the AVHRR 3.7 mm sensors on board the TIROS-N to NOAA-14 satellites. *International Journal of Remote Sensing*, *23*, 5271–5276.

Dixon, R. K., Brown, S., Houghton, R. A., Solomon, A. M., Trexler, M. C., & Wisniewski, J. (1994). Carbon pools and flux of global forest ecosystems. *Science*, *263*, 185–190.

Dowty, P. R. (1993). *A theoretical study of fire detection using AVHRR Data*. MS. University of Virginia, Charlottesville.

Dozier, J. (1981). A method for satellite identification of surface temperature fields of sub-pixel resolution. *Remote Sensing of Environment*, *11*, 221–229.

ERDAS Inc. (1999). *ERDAS field guide* (5th ed). Atlanta, GA.

Eva, H., & Lambin, E. F. (1998). Burnt area mapping in Central Africa using ATSR data. *International Journal of Remote Sensing*, *19*, 3473–3497.

Flannigan, M. D., & Vonder Haar, T. H. (1986). Forest fire monitoring using NOAA satellite AVHRR. *Canadian Journal of Forest Research*, *16*, 975–982.

Fraser, R. H., Li, Z., & Cihlar, J. (2000). Hotspot and NDVI differencing synergy (HANDS): A new technique for burned area mapping over boreal forest. *Remote Sensing of Environment*, *74*, 362–376.

French, N. H. F., Goovaerts, P., & Kasischke, E. S. (2004). Uncertainty in estimating carbon emissions from boreal forest fires. *Journal of Geophysical Research*, *109*, D14S08.

French, N. H. F., Kasischke, E. S., Stocks, B. J., Mudd, J. P., Martell, D. L., & Lee, B. S. (2000). Carbon release from fires in the North American boreal forest. In E. S. Kasischke, & B. J. Stocks (Eds.), *Fire, climate change, and carbon cycling in the boreal forest* (pp. 377–388). New York: Springer-Verlag.

French, N. H. F., Kasischke, E. S., & Williams, D. G. (2002). Variability in the emission of carbon-based trace gases from wildfire in the Alaska boreal forest. *Journal of Geophysical Research*, *107*, 8151.

Goldammer, J. G., & Stocks, B. J. (2000). Eurasian perspective of fire: Dimension, management, policies, and scientific requirements. In E. S. Kasischke, & B. J. Stocks (Eds.), *Fire, climate change, and carbon cycling in the North American boreal forest* (pp. 49–65). New York: Springer-Verlag.

Grégoire, J. -M., Tansey, K., & Silva, J. M. N. (2003). The GBA2000 initiative: Developing a global burned area database from SPOT-VEGETATION imagery. *International Journal of Remote Sensing*, *24*, 1369–1376.

Gutman, G., Elvidge, C., Csiszar, I., & Romanov, P. (2001). NOAA archives of data from meteorological satellites useful for fire products. In F. Ahern, J. Goldammer, & C. O. Justice (Eds.), *Global and regional wildfire monitoring from space: Planning a coordinated international effort* (pp. 257–266). The Hague, The Netherlands: SPB Academic Publishing.

Hansen, M., DeFries, R., Townshend, J. R. G., & Sohlberg, R. (2000). Global land cover classification at 1 km resolution using a decision tree classifier. *International Journal of Remote Sensing*, *21*, 1331–1365.

Hewson, J. H., Trigg, S. N., Loboda, T., Sukhinin, A. I., Czisar, I., & Kasischke, E. S. (in preparation). *Quality assessment of an AVHRR-based fire detection and burned area product for Eastern Russia*.

Hicke, J. A., Asner, G. P., Kasischke, E. S., French, N. H. F., Randerson, J. T., Stocks, B. J., et al. (2003). Postfire response of North American net primary productivity analyzed with satellite observations. *Global Change Biology*, *9*, 1145–1157.

Hudson, R. D. (1969). *Infrared system engineering.* Infrared Laboratories, Hughes Aircraft Company, Wiley Interscience, New York.

Justice, C. O., Giglio, L., Korontzi, S., Owens, J., Morisette, J. T., Roy, D., et al. (2002). The MODIS fire products. *Remote Sensing of Environment*, *83*, 244–262.

Justice, C. O., Kendall, J. D., Dowty, P. R., & Scholes, R. J. (1996). Satellite remote sensing of fires during the SAFARI campaign using NOAA advanced very high resolution radiometer. *Journal of Geophysical Research*, *101*, 23851–23863.

Kajii, Y., Kato, S., Streets, D. G., Tsai, N. Y., Shvidenko, A., Nilsson, S., et al. (2002). Boreal forest fires in Siberia in 1998: Estimation of area burned and emissions of pollutants by advanced very high resolution radiometer satellite data. *Journal of Geophysical Research*, *107*, 4745.

Kasischke, E. S. (2000). Boreal ecosystems in the carbon cycle. In E. S. Kasischke, & B. J. Stocks (Eds.), *Fire, climate change, and carbon cycling in the North American boreal forest* (pp. 19–30). New York: Springer-Verlag.

Kasischke, E. S., & Bruhwiler, L. M. (2002). Emissions of carbon dioxide, carbon monoxide and methane from boreal forest fires in 1998. *Journal of Geophysical Research*, *107*, 8146.

Kasischke, E. S., & French, N. H. F. (1995). Locating and estimating the areal extent of wildfires in Alaskan boreal forests using multiple-season AVHRR NDVI composite data. *Remote Sensing of Environment*, *51*, 263–275.

Kasischke, E. S., Hewson, J. H., Stocks, B. J., van der Werf, G., & Randerson, J. T. (2003). The use of ATSR active fire counts for estimating relative patterns of biomass burning—A study from the boreal forest region. *Geophysical Research Letters*, *30*, ASC10-1–ASC10-4.

Kasischke, E. S., Hyer, E. Novelli, P., Bruhwiler, L., French, N. H. F., Sukhinin, A. I., Hewson, J. H., et. al. (in review). Influences of boreal fire emissions on Northern Hemisphere atmospheric carbon and carbon monoxide, *Global Biogeochemical Cycles*.

Kasischke, E.S., & Penner, J.E. (2004). Improving global estimates of atmospheric emissions from biomass burning. *Journal of Geophysical Research*, *109*, D14501. doi:10.1029/2004JD004972.

Kasischke, E. S., Williams, D., & Barry, D. (2002). Analysis of the patterns of large fires in the boreal forest region of Alaska. *International Journal of Wildland Fire*, *11*, 131–144.

Kidwell, K. B. (1998). NOAA polar orbiter data users guide. Washington, DC: National Oceanic and Atmospheric Administration.

Korovin, G. N. (1996). Analysis of distribution of forest fires in Russia. In J. G. Goldammer, & V. V. Furyaev (Eds.), *Fire in ecosystems of boreal Eurasia* (pp. 112–128). Dordrecht, The Netherlands: Kluwer Academic Publishers.

Kurnaev, S. F. (1990). Forest-vegetation regionalisation. In. *Research and Surveying Institute* '*SoyuzGiproLesKhoz*' *of the USSR State Committee for Forests*. Digitised at the Centre for Agroecological Problems, V.V. Dokuchaev Soil Institute, Russian Academy of Agriculture. http://www.grida.no/prog/polar/ecoreg/ecoap1c.htm

Kukuev, Y. A., Krankina, O. N., & Harmon, M. E. (1997). The forest inventory system in Russia: A wealth of data for western researchers. *Journal of Forestry*, *95*, 15–20.

Li, Z., Nadon, S., & Cihlar, J. (2000). Satellite-based detection of Canadian boreal forest fires: Development and application of the algorithm. *International Journal of Remote Sensing*, *21*, 3057–3069.

Li, Z. Q., Cihlar, J., Moreau, L., Huang, F. T., & Lee, B. (1997). Monitoring fire activities in the boreal ecosystem. *Journal of Geophysical Research*, *102*, 29611–29624.

Lloyd, I. M. (1975). *Thermal imaging systems*. New York: Plenum Press.

Loupian, E. A., Mazurov, A. A., Flitman, E. V., Ershov, D. V., Korovin, G. N., Novik, V. P., et al. (in press). Satellite monitoring of forest fires in Russia at federal and regional levels. *Mitigation and Adaptation Strategies for Global Change*, accepted by guest editors.

Matson, M., & Dozier, J. (1981). Identification of subresolution high temperature sources using a thermal IR sensor. *Photogrammetric Engineering and Remote Sensing*, *47*, 1311–1318.

Olson, J. R., Baum, B. A., Cahoon, D. R., & Crawford, J. H. (1999). Frequency and distribution of forest, savanna, and crop fires over tropical regions during PEM-Tropics A. *Journal of Geophysical Research-Atmospheres*, *104*, 5865–5876.

Razafimpanilo, H., Frouin, R., Iacobellis, S. F., & Somerville, R. C. J. (1995). Methodology for estimating burned area from AVHRR reflectance data. *Remote Sensing of Environment*, *54*, 273–289.

Remmel, T. K., & Perera, A. H. (2001). Fire mapping in a northern boreal forest: Assessing AVHRR/NDVI methods of change detection. *Forest Ecology and Management*, *152*, 119–129.

Rosell, F. A., & Wilson, R. H. (1973). Ch. 5, recent physical experiments and the display signal-to-noise ratio concept. In L. M. Biberman (Ed.), *Perception of displayed information*. Plenum.

Roy, D. P., Lewis, P. E., & Justice, C. O. (2002). Burned area mapping using multi-temporal moderate spatial resolution data—A bi-directional reflectance model-based expectation approach. *Remote Sensing of Environment*, *83*, 263–286.

Seiler, W., & Crutzen, P. J. (1980). Estimates of gross and net fluxes of carbon between the biosphere and atmosphere. *Climatic Change*, *2*, 207–247.

Shugart, H. H., Leemans, R., & Bonan, G. B. (1992). *A systems analysis of the global boreal forest*. Cambridge: Cambridge University Press.

Shvidenko, A., & Goldammer, J. G. (2001). *Fire situation in Russia.* Pages 41–59 In Issue No. 24, International Forest Fire News. United Nations Economic Commission for Europe, Food and Agriculture Organization.

Shvidenko, A., & Nilsson, S. (2002). Dynamics of Russian forests and the carbon budget in 1961–1998: An assessment based on long-term forest inventory data. *Climatic Change*, *55*, 5–37.

Shvidenko, A. Z., & Nilsson, S. (2000). Extent, distribution, and ecological role of fire in Russian forests. In E. S. Kasischke, & B. J. Stocks (Eds.), *Fire, climate change, and carbon cycling in the North American boreal forest* (pp. 132–150). New York: Springer-Verlag.

Siegert, F., & Hoffmann, A. A. (2000). The 1998 forest fires in East Kalimantan (Indonesia): A quantitative evaluation using high resolution, multitemporal ERS-2 SAR images and NOAA-AVHRR hotspot data. *Remote Sensing of Environment*, *72*, 64–77.

Simon, M., Plummer, S., Fierens, F., Hoelzemann, J.J., & Arino, O. (2004). Burnt area detection at global scale using ATSR-2; the GLOBSCAR products and their qualifications. *Journal of Geophysical Research*, *109*, D14502. doi:10.1029/2003JD003622.

Sofronov, M. A., Volokitina, A. V., & Shvidenko, A. Z. (1998). Wildland fires in the north of Central Siberia. *Commonwealth Forestry Review*, *77*, 124–127.

Soja, A. J., Cofer, W. R., Shugart, H. H., Sukhinin, A. I., Stackhouse Jr., P. W., McRae, D. J., et al. (2004a). Estimating fire emissions and disparities in boreal Siberia (1998 through 2002). *Journal of Geophysical Research*, (2004jd007540).

Soja, A. J., Sukhinin, A., Cahoon Jr., D. R., Shugart, H. H., & Stackhous Jr., P. W. (2004b). AVHRR-derived fire frequency, distribution, and area burned in Siberia. *International Journal of Remote Sensing*, *25*, 1939–1951.

Stocks, B. J. (1991). The extent and impact of forest fires in northern circumpolar countries. In J. S. Levine (Ed.), *Global biomass burning: Atmospheric, climatic, and biospheric implications* (pp. 198–202). Cambridge, MA: MIT Press.

Stocks, B. J., Mason, J. A., Todd, J. B., Bosch, E. M., Wotton, B. M., Amiro, B. D., et al. (2002). Large forest fires in Canada, 1959–1997. *Journal of Geophysical Research*, *107*, 8149.

Stolbovoi, V. (2002). Carbon in Russian soils. *Climatic Change*, *55*, 131–156.

Stolbovoi, V., & McCallum, I., 2002. *CD-ROM* "*Land Resources of Russia*". International Institute for Applied Systems Analysis and the Russian Academy of Science, Laxenburg, Austria.

Stroppiana, D., Pinnock, S., & Gregoire, J. -M. (2000). The global fire product: Daily fire occurrence from April 1992 to December 1993 derived from NOAA AVHRR data. *International Journal of Remote Sensing*, *21*, 1279–1288.

Sukhinin, A. I. (2003). Russian Federation Fire 2002 Special: Part III. The 2002 fire season in the Asian part of the Russian federation. *International Forest Fire News*, *28*.

Tansey, K., Grégoire, J.-M., Stroppiana, D., Sousa, A., Silva, J.M.N., Pereira, J.M.C., et al. (2004). Vegetation burning in the year 2000: Global burned area estimates from SPOT VEGETATION data. *Journal of Geophysical Research*, *109*, D14503. doi:10.1029/2003JD003598.

Valendik, E. N. (1996). Temporal and spatial distribution of forest fires in Siberia. In J. G. Goldammer, & V. V. Furyaev (Eds.), *Fire in Ecosystems of Boreal Eurasia* (pp. 129–138). Dordrecht: Kluwer Academic Publishers.

Van Cleve, K., Chapin III, F. S., Flanagan, P. W., Viereck, L. A., & Dyrness, C. T. (1986). *Forest ecosystems in the Alaskan taiga*. New York: Springer-Verlag.

Van der Werf, G. R., Randerson, J. T., Collatz, G. J., Giglio, L., Kasibhatla, P. S., Arellano, A., et al. (2004). Continental-scale partitioning of fire emissions during the 97/98 El Nino. *Science*, *303*, 73–76.

Warren, S. G., Hahn, C. J., London, J., Chervin, R. M., & Jenne, R. L. (1986). *Global distribution of total cloud cover and cloud type amounts over land*. National Center for Atmospheric Research, Boulder.